



HAL
open science

Competing stacking modes in crystals of trihalogeno-trimethyl-benzene Theory meets experiment

J. Meinnel, A. Amar, A. Boucekkine, O. Jeannin, F. Camerel, F. Barrière

► **To cite this version:**

J. Meinnel, A. Amar, A. Boucekkine, O. Jeannin, F. Camerel, et al.. Competing stacking modes in crystals of trihalogeno-trimethyl-benzene Theory meets experiment. *Journal of Crystal Growth*, 2019, 515, pp.1-8. 10.1016/j.jcrysgr.2019.03.006 . hal-02090000

HAL Id: hal-02090000

<https://univ-rennes.hal.science/hal-02090000>

Submitted on 6 Jun 2019

HAL is a multi-disciplinary open access archive for the deposit and dissemination of scientific research documents, whether they are published or not. The documents may come from teaching and research institutions in France or abroad, or from public or private research centers.

L'archive ouverte pluridisciplinaire **HAL**, est destinée au dépôt et à la diffusion de documents scientifiques de niveau recherche, publiés ou non, émanant des établissements d'enseignement et de recherche français ou étrangers, des laboratoires publics ou privés.

Competing Stacking Modes in Crystals of Trihalogeno-Trimethyl-Benzene: Theory Meets Experiment.

Jean Meinnel^{1#}, Anissa Amar^{1,2}, Abdou Boucekkine^{*1}, Olivier Jeannin¹, Franck Camerel¹, Frédéric Barrière¹

1- Univ Rennes, CNRS, ISCR - UMR 6226, F-35000 Rennes, France

2- Département de chimie, Faculté des sciences, UMMTO, 15000 Tizi-Ouzou, Algeria and Laboratoire de thermodynamique et modélisation moléculaire, Faculté de chimie, USTHB, 16111 Bab Ezzouar, Alger, Algeria

Tribute to Emeritus Professor Jean Meinnel who directed the study until his death on August 5th 2018, at 92 years old.

Abstract:

The special case of the stacking of trihalogeno mesitylene (TXM) molecules has been investigated. Below 300 K, these molecules lead to needle shaped crystals in a triclinic arrangement. Thanks to DFT computations and an empirical atom-atom interaction model this packing mode has been rationalized. Aggregates of TXM molecules differently packed have been considered, namely dimers and trimers of type A, the molecules being piled one over the other along the axis **a**, and dimers B and trimers B, the molecules lying in the same **bc** plane. From the computations, it appears that the stabilizing energy of formation of a dimer of two molecules piled along **a** is several times larger than the energy gain obtained from the formation of a dimer of two neighbors in the **bc** plane. It has also been found that the energy of formation of a trimer of type A is approximately twice the energy of formation of a dimer A, so that an additive rule occurs. These conclusions are in perfect agreement with the experimental observations of the shape of the crystals obtained by crystallization from a super-saturated solution of TXM in an organic solvent: long needles with TXM molecules stacked along the axis **a** have always been obtained and never thin plate-like crystals.

Keywords: A1-Computer simulation; A1-Crystal structure; A1-Growth models; A2-Single crystal growth; A2-Growth from solutions; B1-Aromatic compounds

Introduction:

Investigating the nature and the role of the intermolecular interactions which drive molecular stacking in crystals is of importance especially for crystal engineering.

Among the different possible driving forces at work in the interaction between substituted benzenes, van der Waals (vdW) interactions, π - π stacking or hydrogen bonding in some cases, have been pointed out. In the case of benzene derivatives bearing halogen substituents, the influence of halogen-halogen contacts (since the X...X distance could be shorter than twice the vdW radii) and halogen bonding have also been cited.

We are interested in the special case of the stacking of trihalogeno mesitylene (TXM) molecules. The latter species exhibit a dipole moment almost equal to zero. Below 300 K, these molecules are packed in such a way that they lead to needle shaped crystals in a triclinic arrangement. To shed light on the origin of such crystal structures, we investigate theoretically different possible packing modes, considering several sets of molecules, using two theoretical approaches, namely Density Functional Theory (DFT) computations and an empirical atom-atom interaction model. The computations of the packing energies and of the optimized geometries of the considered molecular clusters are carried out to assist the understanding of the observed stackings. Furthermore, new crystallographic and thermal analyses are carried out.

Previous works on halogenomethylbenzenes

As early as 1940 [1], researchers at Bell Telephone laboratories were interested by hexa-substituted benzenes (HSB) of general formula $C_6X_nMe_{(6-n)}$ containing both halogen atoms and methyl groups ($X = Cl, Br, I$ and $Me = CH_3$, n varying from 0 to 6) because of their relatively high dielectric static constant at room temperature in the solid state. The large permittivity found at 300 K for frequencies larger than 10kHz and even 1 MHz, is explained by the possibility for the molecules to rotate by 60° steps, leading to the characteristic Debye absorption-dispersion phenomenon. The validity of this hypothesis of an orientational dynamic disorder was confirmed in 1958 by the X-Ray Diffraction (XRD) determination of the crystal structure of the 1,2-dichloro-3,4,5,6-tetramethylbenzene (dCtMB) [2] at room temperature. The crystal is monoclinic and the space group is $P2_1/n$ with 2 “mean” disordered molecules per cell. In the seventies, the structures of several other HSB were studied, all of them were found to be disordered [3-6] within the space group $P2_1/n$. At the same time, two European groups have systematically studied HSB by proton nuclear magnetic resonance and dielectric susceptibility in the 70-320 K temperature range [6-10]. They established that what Kitaigorodski called the “rotational crystalline state” was widespread [11]. In this state, the “quasi hexagonal” discotic molecules are rotating by of 60 or 120° steps into their molecular plane at frequencies often larger than 1 MHz while an ordering in a static state is appearing below 150 K [3, 9, 10]. Amazingly, until 1995 no work has been done to establish the structure of the symmetrical trihalogeno-mesitylenes congeners $C_6X_3Me_3$ (or TXM). Our group, in the period 1995-2002, has established that below room temperature, TXM compounds crystallize in the $P-1$ triclinic group without any apparent disorder and not in the monoclinic group like the others HSB. The structure of the trichloro-mesitylene (TCM) at 150 and 297 K was solved by XRD [12], that of the tribromo-mesitylene (TBM) was solved at 295 K by XRD [13] and at 14 K by neutron diffraction (ND) [14] while that of the triiodo-mesitylene (TIM) was solved at 293 K by XRD [15] and at 15 K by ND [16].

So below 300 K, these TXM molecules are always packed in a triclinic arrangement and stacked as pancakes along the oblique axis **a**, giving crystals with a needle shape (Figure 1). The molecular plane lies practically into the **bc** plane (deviation smaller than 5°) forming a quasi-hexagonal arrangement characterized by halogen synthons: Cl_3 , Br_3 or I_3 but also $(CH_3)_3$ synthons (Figure 2). The planar **bc** layers are stacked in an antiparallel manner along the axis **a**. This triclinic arrangement below room temperature was confirmed later by XRD [17] and ND experiments [18]. The Figures 1 and 2 give two projections of the common structure. Figure 1 is a projection on the **ab** plane and Figure 2 the projection on the **bc** plane in the case of the TIM at 293 K. In fact, the case of TCM is a little more complicated: from X-ray [12, 18] and calorimetric measurements [19, 20] it has been

established that below 300 K, TCM exhibits two different triclinic crystal phases differing only by translations of the molecules in the *bc* plane while there is a “sluggish” transition around 160 K. To summarize, at temperatures below 160 K, TCM, TBM and TIM, are rigorously isostructural, irrespective of the nature of the methyl group (CH₃ or CD₃) as shown in Table 1. However, no experiments have been done above room temperature and in consequence only partial information was available to draw general conclusions regarding the structures of TXM species in the solid state.

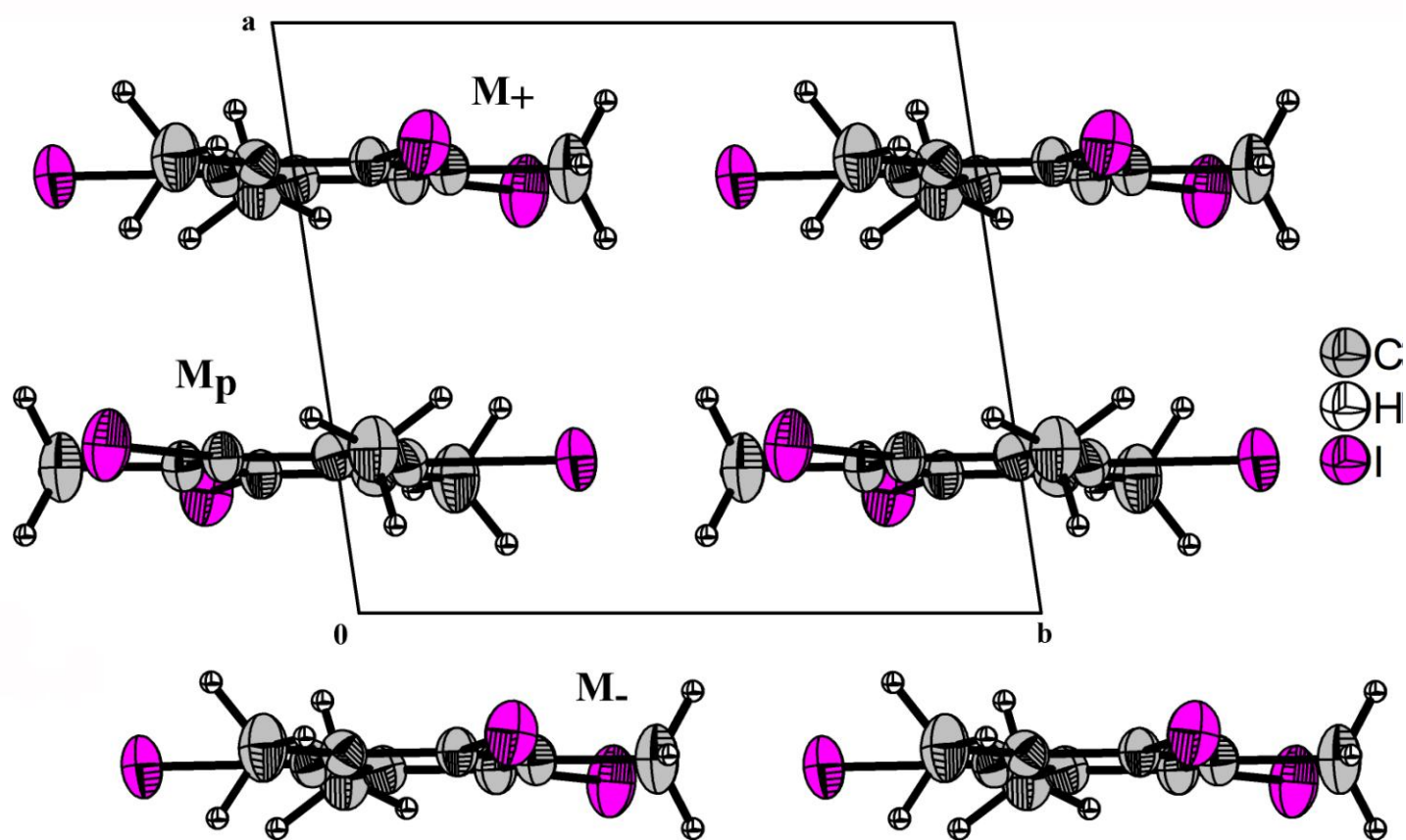


Figure 1- Projection of the TIM unit cell along *c*, onto the *ab* plane. Displacement ellipsoids are shown at the 50% level probability. Structure obtained at 293 K.

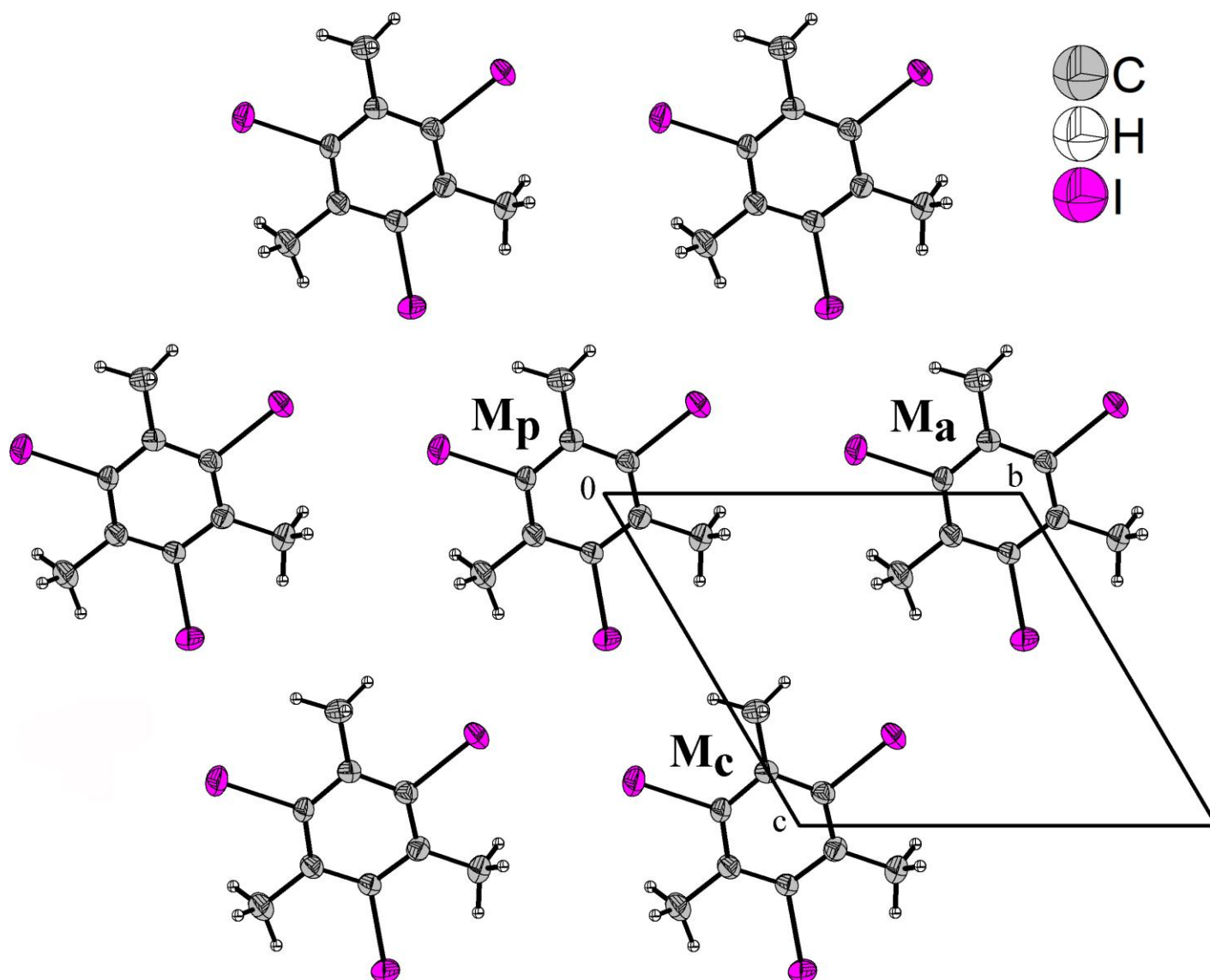


Figure 2- Projection onto the *bc* plane showing six TIM molecules.

Table 1 – Crystal cell parameters for $C_6X_6(CH_3)_{6-n}$ using the convention $a < b < c$ and $60^\circ < \text{angles} < 90^\circ$ for the triclinic cell even if another convention was used in the published papers. For comparison data for two symmetrical hexa-halogeno-benzenes $C_6Cl_3I_3$ and $C_6Br_3I_3$ are also tabulated.

| Mat | $C_6Cl_3(CH_3)_3$ | $C_6Cl_3(CH_3)_3$ | $C_6Br_3(CD_3)_3$ | $C_6Br_3(CD_3)_3$ | $C_6Br_3(CH_3)_3$ | $C_6Br_3(CH_3)_3$ | $C_6I_3(CH_3)_3$ | $C_6Cl_3I_3$ | $C_6Br_3I_3$ |
|----------|-------------------|-------------------|-------------------|-------------------|-------------------|-------------------|------------------|--------------|--------------|
| SG | P-1 | P-1 | P-1 | P-1 | P-1 | P-1 | P-1 | P-1 | P-1 |
| a | 7.42872 | 7.646 | 7.58647 | 7.78653 | 7.692 | 7.810 | 8.0486 | 7.7131 | 7.9452 |
| b | 8.75731 | 8.789 | 9.03555 | 9.09463 | 9.0616 | 9.107 | 9.6105 | 9.4269 | 9.4962 |
| c | 8.78729 | 8.836 | 9.03867 | 9.13630 | 9.0943 | 9.153 | 9.6204 | 9.4299 | 9.5119 |
| α | 59.9255 | 60.110 | 60.1626 | 59.9963 | 60.0242 | 60.005 | 60.1766 | 60.213 | 60.137 |
| β | 68.0817 | 68.019 | 67.6250 | 67.9840 | 67.7702 | 67.990 | 66.7586 | 66.116 | 66.202 |
| χ | 85.0854 | 85.085 | 85.2869 | 84.9905 | 84.9090 | 84.998 | 85.3542 | 85.575 | 85.512 |

| | | | | | | | | | |
|-----|--------|--------|--------|--------|-------|-------|--------|--------|--------|
| V | 455.78 | 467.10 | 492.53 | 512.66 | 502.4 | 515.9 | 586.97 | 537.43 | 562.51 |
| T | 2 K | 293 K | 4 K | 290 K | 173 K | 293 K | 293 K | 100 K | 100 K |
| ref | 17 | 12 | 17 | 17 | 16 | 13 | 14, 15 | 18 | 18 |

New crystallographic and differential thermal analysis data on trihalogenomesitylenes.

In order to have a complete overview of the thermal history of TXM compounds, Differential Scanning Calorimetry (DSC) experiments have been performed from 223 K up to 513 K (Figure 3 and Figures S1 and S2 in Supporting Information SI). TCM and TBM were found to melt into an isotropic phase at 484 K and 499 K, respectively, whereas TIM compounds melt at much lower temperature around 433 K. The melting of the compounds into an isotropic phase was confirmed by polarized optical microscopy investigations. The melting transitions are also associated to high enthalpy values around 30 to 50 J.g⁻¹. A phase change from an ordered triclinic to a disordered monoclinic structure was also observed around 319.5 K for TCM, 362.5 K for TBM and 327.5 K for TIM. This crystal-crystal transition requires far less energy and the transition enthalpies are found to lie around 3-5 J.g⁻¹. Temperature-dependent X-ray diffraction experiments performed on TCM single crystal upon heating confirm the presence of a phase transition between 315 and 320 K. Below 315K, the compound crystallizes into a triclinic unit cell ($a = 7.7907 \text{ \AA}$, $b = 8.8483 \text{ \AA}$, $c = 8.8782 \text{ \AA}$, $\alpha = 119.3439^\circ$, $\beta = 107.1781^\circ$, $\gamma = 96.1198^\circ$, $\text{vol} = 485.923 \text{ \AA}^3$ at 315K), whereas, above 320K, the compound crystallizes into a monoclinic unit cell ($a = 8.2578 \text{ \AA}$, $b = 3.8981 \text{ \AA}$, $c = 14.2567 \text{ \AA}$, $\beta = 94.0246^\circ$, $\text{vol} = 457.784 \text{ \AA}^3$, at 320 K). Unfortunately, the crystal structure of the TCM compound in the monoclinic crystal system could not be solved due to the appearance of cracks in the crystal above 320K.

A second thermal anomaly between two disordered phases also occurs at 396 K for TCM and 456 K for TBM (Figure 3). This second transition is not observed with TIM but it cannot be excluded that this transition is concomitant with the first crystal-crystal phase transition considering the broadness of the peak observed with TIM. Furthermore, from solid state NMR studies, it may be concluded that the disorder in these high temperature phases corresponds to rotation of TXM molecules by steps equal to 60° around the “quasi-hexagonal” axis perpendicular to their molecular plane, the rotation occurs at frequencies in the megahertz to gigahertz ranges. Thus, TXM does not behave differently from other HSB contrarily to what was thought by several authors [17, 21, 22], but these compounds also show a phase transition between an ordered triclinic phase and a disordered monoclinic phase in which the molecules rotate around their three-fold axis but at higher temperatures.

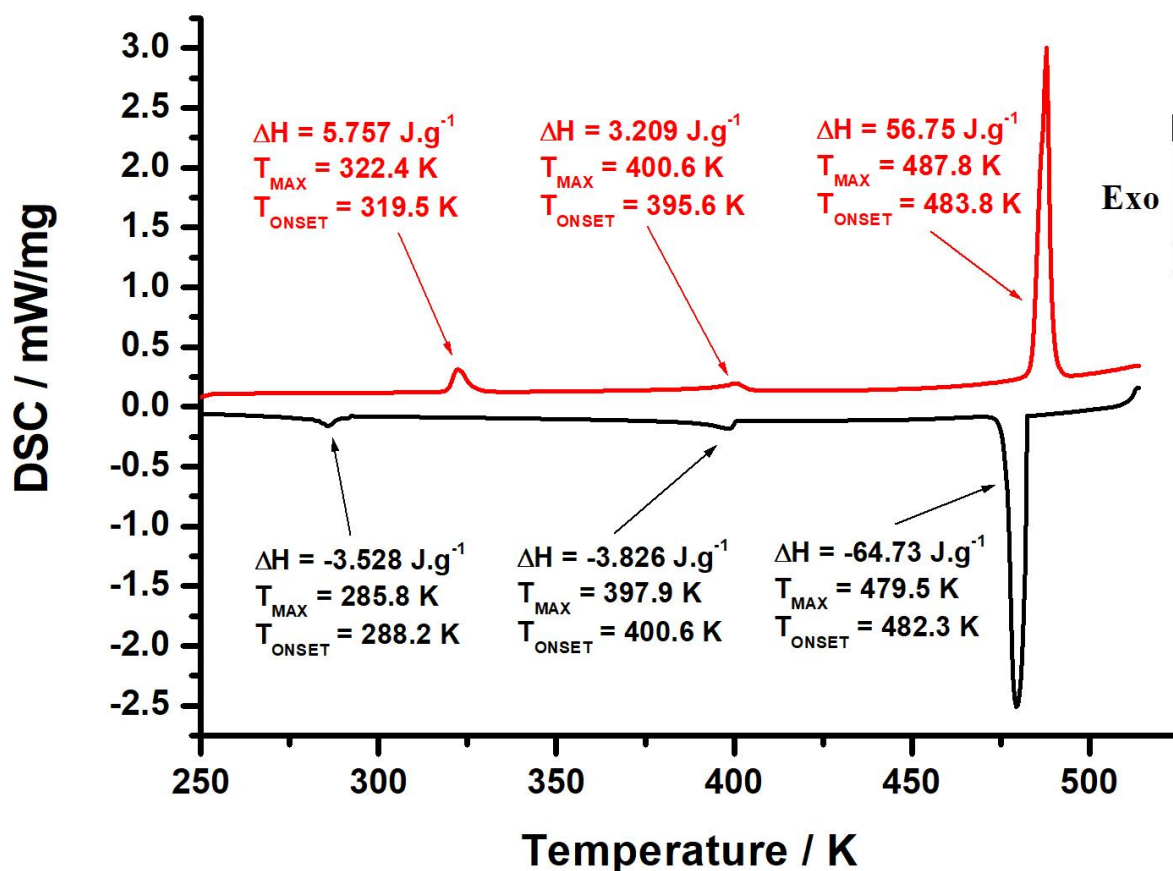


Figure 3- Result of a DSC analysis for TCM. The sample was quenched at 248 K, then warmed until 513 K at a speed of 10 K per minute and then cooled to 248 K.

About the conclusions on the halogen-halogen interactions previously drawn from studies of halogeno-aromatic crystal structures.

In 1994, examining the nature of Cl...Cl intermolecular interactions Price and al. [23] reported that in 1971 Green and Schmidt [24] had found that dichloro-substitution on aromatic molecules tends to yield crystals with a short axis around 4 Å. They extended this observation and mentioned the possibility for halogen atoms to play a specific role in what they call "Crystal Engineering". In 1989, Desiraju [21] examining the consequences of X...X close contacts in the crystals structure of polyhalogeno-aromatics, emphasized that "the role of halogen-halogen (X...X) contacts within crystal structures is to stabilize two-dimensional motifs which may in turn stack to form the 4 Å short axis". He concluded that these two-dimensional motifs give rise, in monoclinic structures, to corrugated sheets or linear ribbons. Desiraju added "it is even possible to reverse the argument to adopt the 4 Å structure for chloro-aromatics, the molecule must be planar, have a large number of halogen substituents, and lack other stronger substitutions". He concluded that "the most problematic aspect

of crystal structure prediction of halogen-atom containing compounds is that there is a complex interplay between several weak, variably directional forces, probably X...X contacts are most effective when they compete only with van der Waals forces". Desiraju and Parthasarathy [25] have also examined the question of local geometrical problems: what is the preferred direction of approach of an electrophile or nucleophile atom around the carbon halogen bond? They have proposed to name I and II the two different types C-X...X-C contacts observed in the local geometry. The angles characterizing the X...X interactions are named respectively θ_1 for the angle C-X₁...X₂ and θ_2 for X₁...X₂-C; in type I geometry, $\theta_1 = \theta_2 \sim 160^\circ$ (head-on approach) and in type II, θ_1 is nearly 170° and θ_2 nearly 90° (side-on approach). They said that in type I identical portions of the halogen atoms make the nearest approach, whereas the variation in the X...X distances is due to the elliptical shape of the halogen atoms as proposed by Nyburg and Faerman [26] for chlorine, which has a minor radius $r_{\min} = 1.58 \text{ \AA}$ for head-on approach ($\theta = 180^\circ$) and a major radius $r_{\max} = 1.78 \text{ \AA}$ for a side-on approach ($\theta = 90^\circ$). This is in agreement with the fact that the majority of the Cl...Cl contacts in chlorinated hydrocarbons is smaller than twice the spherical (vdW) Waals radius *i.e.* 3.52 \AA . This geometrical anisotropy results of an anisotropic distribution of the electron density [27-29] named polar flattening [17, 29, 30], the chlorine atom showing an electropositive crown in the polar region along the C-Cl axis surrounded by an electroneutral ring and further out, an electronegative belt in the equatorial region.

The triclinic packing is restricted to molecules that have a symmetrical (1,3,5- and 2,4,6-) halogen substitution pattern. In the triclinic structure, the planar molecules form π - π stacks; within these stacks the molecules are 3.44 \AA apart (perpendicular distance) (Figure 1). The close packing of these stacks is characterized by specific, polarization induced X...X interactions that result in the formation of threefold-symmetrical X₃ synthons, this leads to a layered pseudo-hexagonal structure in the **bc** plane (Figure 2). As can be seen in Figure 2 and in Table 2, the halogen-halogen interactions is intermediary between a head-on approach ($\theta = 180^\circ$) and a side-on approach ($\theta = 90^\circ$) in the **bc** planes for the TXM compounds. The triclinic packing can also be viewed as a stacking layered pseudo-hexagonal structures in which successive planar layers are inversion related in a space-filling manner. Regarding the comparison between interatomic distances and angles from the XRD measurements and the DFT computational results in Table 2, it can be seen that the agreement is satisfactory only for chlorine and not for bromine or iodine. However, it is worth reminding that the XRD values refer to the whole crystals whereas the DFT values are computed for dimers and trimers models. It is likely that the packing effects are more important in the case of the heaviest halogen atoms. Interestingly, when considering the distances between the centroids of the rings a rather good agreement is observed between the XRD and the DFT values. Indeed, the average XRD distance between the benzene rings centroids is respectively equal to 3.83 , 3.94 and 4.16 \AA for TCM, TBM and TIM whereas the DFT values are only 0.11 to 0.17 \AA smaller than the XRD ones. It is worth noting that these short distances are indicative of a strong π - π stacking interaction.

π - π stacking dominates the packing in the triclinic structure but specific X...X interactions should play a role in the triclinic packing, especially in the formation of the pseudo-hexagonal structure in the **bc** plane. Is the crystal packing governed by the π - π stacking or by the formation of X₃ synthon which in turn leads to the formation of the **bc** plane?

To give a quantitative answer to the uncertainty about the origin of the TXM packing energy and particularly in the case of the triclinic arrangement, we present two ways of calculating this energy. In the first one, we have extended to clusters the results of standard DFT calculation on an isolated molecule; in the second one, we have used atom-atom semi-empirical interaction parameters to find the van der Waals energy of formation of the same clusters.

Table 2 – Mean halogen-halogen distances (Å) and mean θ_1 and θ_2 angles (°) measured by XRD and computed by DFT for TCM, TBM and TIM.

| | XRD ^a | DFT | XRD ^a | DFT | XRD ^a | DFT |
|-----|------------------|-------|-----------------------|-----------------------|------------------------|------------------------|
| | X...X | X...X | C-X1...X ₂ | C-X1...X ₂ | X1...X ₂ -C | X1...X ₂ -C |
| TCM | 3.575 | 3.711 | 169.97 | 165.537 | 128.14 | 123.750 |
| TBM | 3.627 | 3.984 | 171.39 | 158.508 | 124.61 | 119.330 |
| TIM | 3.929 | 4.480 | 170.38 | 153.186 | 119.41 | 105.015 |

a) TCM, 293 K; TBM, 173 K; TIM, 293 K.

Determination of the energy of stacking of the TXM in the triclinic phase

Energy of formation of dimers or trimers of TXM calculated using DFT computations

In our previous studies on TXM structures, we have determined the molecular conformations at low temperature (14 or 15 K) using ND. This allowed us to determine the precise positions of the atomic nuclei, thus accurate internuclear angles and bond lengths [14, 16 and 18].

DFT calculations have been carried out using different functionals, M062X [31, 32], ω B97X and ω B97XD [33] and a suitably polarized LANL2DZP atomic basis set [34] using the Gaussian09 package [35]. We present only the results obtained with ω B97XD because those obtained with the other functionals lead to similar conclusions. We point out that the ω B97XD functional includes atom-atom dispersion corrections. Geometry optimizations and calculation of the normal modes of vibration have been done for all species, in order to get their total energies including the zero point vibration energy (ZPE).

First, we computed the values for the geometrical parameters and energy E_m of an isolated molecule. A good agreement between the calculated values and those measured by ND is obtained (Table S1 in the SI). Furthermore, the computed vibration frequencies were also found to be in good agreement with the values obtained experimentally.

Then, we extended such DFT calculations to aggregates of TXM molecules, namely dimers and trimers in which the stacked molecules have different relative positions. For the dimers A and trimers A, the molecules are piled one over the other along the axis **a**, one dimer A corresponds to the pair $M_p + M_+$ of the Figure 1; its energy of formation is E_{DA} and comparison with 2 times E_m allows to estimate the packing energy of DA. Trimer A corresponds to a trio like $M. + M_p + M_+$ (see Figure 1); its calculated energy of formation E_{TA} is compared to three times E_m . Dimer B and trimer B correspond to molecules lying in the plane **bc** (Figure 2). DB is the pair $M_p + M_A$ or the pair $M_p + M_C$ and its

energy of formation is E_{DB} . The trimer B is $M_p + M_A + M_B$ of energy E_{TB} (Table 3). The optimized geometries of the DA and DB dimers of TBM are given in the SI (Table S2) as well as the optimized coordinates of all species in Table S3, whereas their structures are displayed in Figure 4.

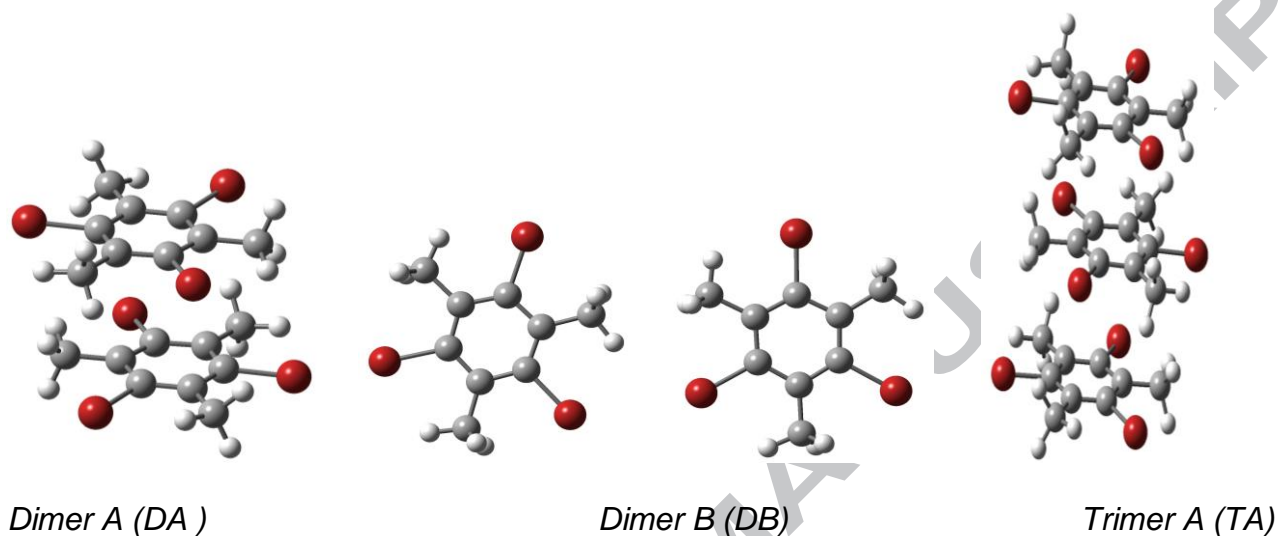


Figure 4 – Optimized geometries of DA, DB and TA

Table 3- ω B97XD DFT energies (Hartree Ha and kJ/mol) of formation of dimers and trimers along **a** and in the **bc** plane.

| Cluster | Energy +ZPE | TCM | TBM | TIM |
|-------------------|------------------|-----------|-----------|-----------|
| Mono: | E_m | -393.049 | -387.680 | -382.319 |
| Dimer A: DA | E_{DA} | -786.117 | -775.381 | -764.662 |
| Dimer B: DB | E_{DB} | -786.100 | -775.363 | -764.641 |
| 2 separate M: 2 M | $2.E_m$ | -786.098 | -775.360 | -764.638 |
| DA – 2M(Ha) | $E_{DA} - 2.E_m$ | -0.019 | -0.021 | -0.024 |
| DA – 2M (kJ/mol) | $E_{DA} - 2.E_m$ | -49.9 | -55.1 | -63.0 |
| DB – 2M (Ha) | $E_{DB} - 2.E_m$ | -0.002 | -0.003 | -0.003 |
| DB – 2M (kJ/mol) | $E_{DB} - 2.E_m$ | -5.3 | -7.9 | -7.9 |
| Trimer A: TA | E_{TA} | -1179.187 | -1163.084 | -1147.004 |

| | | | | |
|---------------------|---------------------|-----------|-----------|-----------|
| 3 separate M: 3 M | $3.E_m$ | -1179.147 | -1163.040 | -1146.957 |
| TA – TM (Ha) | $E_{TA} - 3.E_m$ | -0.040 | -0.044 | -0.047 |
| TA – TM (kJ/mol) | $E_{TA} - 3.E_m$ | -105.0 | -115.5 | -123.4 |
| Trimer B: TB-S1 | E_{TB-S1} | -1179.180 | -1163.072 | -1147.000 |
| TB-S1 – TM (Ha) | $E_{TB-S1} - 3.E_m$ | -0.033 | -0.032 | -0.043 |
| TB-S1 – TM (kJ/mol) | $E_{TB-S1} - 3.E_m$ | -86.6 | -84.0 | -112.9 |
| Trimer B: TB-S2 | E_{TB-S2} | -1179.180 | -1163.079 | -1147.000 |
| TB-S2 – TM (Ha) | $E_{TB-S2} - 3.E_m$ | -0.033 | -0.039 | -0.043 |
| TB-S2 – TM (kJ/mol) | $E_{TB-S2} - 3.E_m$ | -86.6 | -102.4 | -112.9 |
| Trimer B: TB-S3 | E_{TB-S3} | -1179.171 | -1163.069 | -1146.995 |
| TB-S3 – TM (Ha) | $E_{TB-S3} - 3.E_m$ | -0.024 | -0.029 | -0.038 |
| TB-S3 – TM (kJ/mol) | $E_{TB-S3} - 3.E_m$ | -63.0 | -76.1 | -99.8 |

From Table 3, it appears that the increased stabilizing $E_{DA} - 2.E_m$ energy for formation of a dimer with molecules piled along **a** is several times larger than the energy gain $E_{DB} - 2.E_m$ obtained for the formation of a dimer with two neighboring molecules in the **bc** plane. Interestingly, it can be seen that the energy difference $E_{DA} - 2.E_m$ increases when passing from TCM to TBM then to TIM, so that the most polarizable halogen, *i.e.* iodine, leads to the most stable dimer stacked along **a**.

It can be seen that the energy of formation of a trimer TA is approximately twice the energy of formation of a dimer DA so that an additive rule occurs. It is worth noting that taking into account the counterpoise correction when computing the bonding energies in the case of dimers DA or DB, it is found that this correction has a small effect on the bonding energy so that it can be neglected.

The planar TB configuration is not stable at our level of DFT calculations. Indeed, when optimizing the geometry of TB trimers, starting from three in plane molecules as described above, the three molecules do not remain in the same plane but move on to give either a DA stacked dimer, the third molecule being perpendicular to this dimer or to give three molecules facing to each other with the centers of the benzene rings approximately placed on the vertices of a triangle (the 3 obtained structures S1, S2 and S3 given in Figure 6). If the geometry optimization is carried out imposing the three rings to be in the same plane, the bonding energy is very low, -10.4 kJ/mol, and the structure is unstable as indicated by the obtained numerous imaginary vibration frequencies. This result is indicative of the fact that in-plane aggregation of TXM molecules is not favored.

The S1, S2 and S3 structures exhibit a smaller bonding energy than the TA one. In the case of TBM, the bonding energies of these forms are respectively equal to -84.0, -102.4 and -76.1 kJ/mol to be compared to that of a TA stacking, *i.e.* -115.5 kJ/mol. So the most stable trimeric species is formed along **a**. The trimer observed in structure S2 is the most stable trimeric species of the three packings.

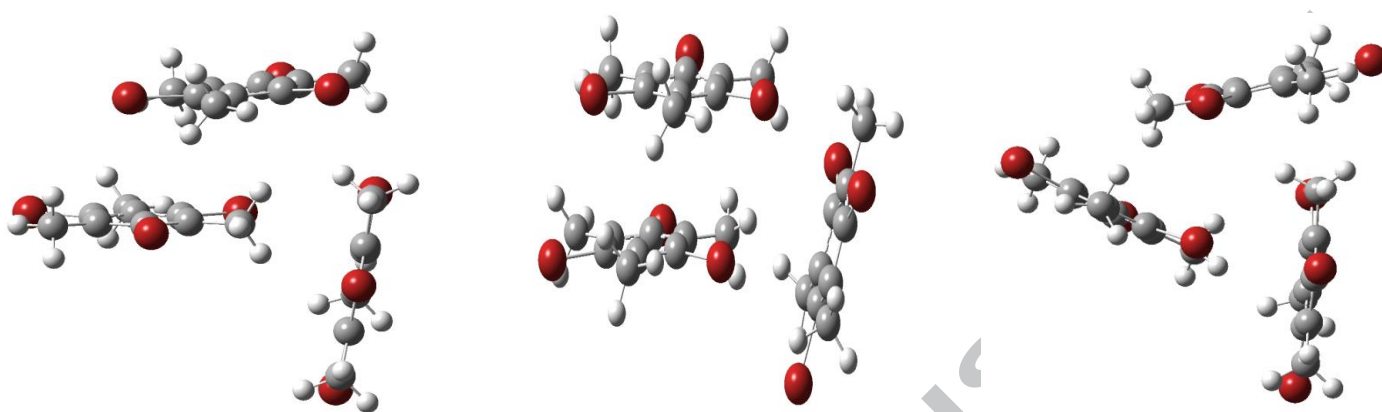


Figure 5 - Structures S1, S2 and S3 (from left to right) of a TB trimer of TCM initially in the *bc* plane

These calculations which may be extended to clusters of more numerous molecules along *a* or in the *bc* plane, demonstrate that the stabilizing energy of uni-dimensional stacking of TXM molecules like pancakes along the axis *a* is larger than that involved to form triangular interactions into a two-dimensional sheet. Experimentally, these conclusions are in perfect agreement with the observations of the shape of the crystals obtained by crystallization from a super-saturated solution of TXM in an organic solvent. Long needles aligned along the axis *a* have always been obtained and never thin plate-like crystals.

Electrostatic surface potential (ESP) calculations may give additional insights into the electrostatic effects driving the crystal arrangements, and particularly shed light on specific interactions. First of all, it can be seen on Figure 6 in the case of an isolated TBM molecule that the ESP is not uniform around the halogen atoms. Indeed the bromine atom is polarized with a large negative lateral belt (red color in Figure 6, top) and a highly positive surface potential localized at the apex of the C-Br bond (blue dot at Br on Figure 6 top, often referred to as a “sigma-hole”).

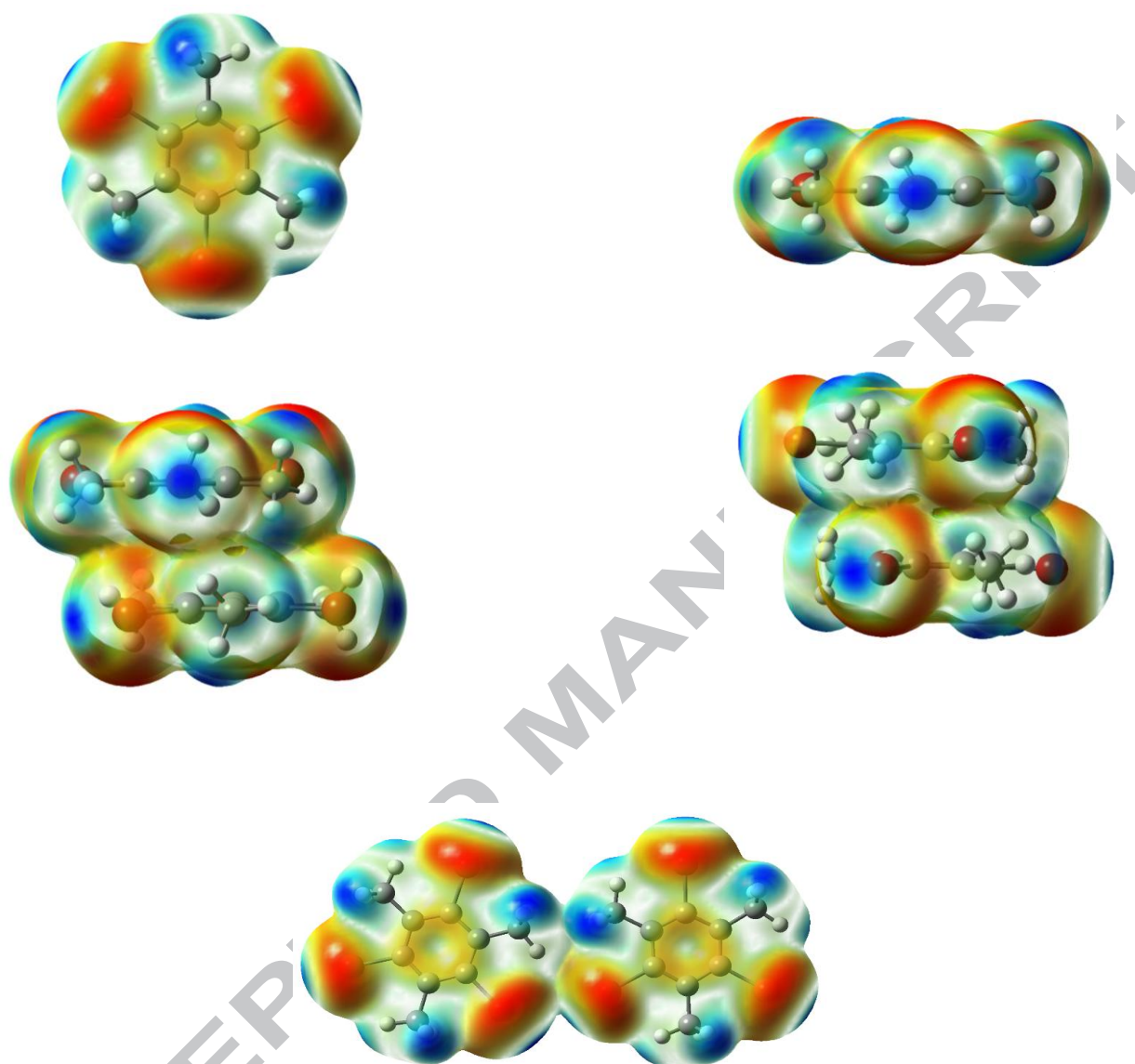


Figure 6: Molecular electrostatic potential surface mapped at the $0.003 \text{ e}^- \cdot \text{au}^{-3}$ isodensity surface, for: Top: two views of TBM, Middle: two views of Dimer A, Bottom: Dimer B. The common color scale ranges from $-9.4 \text{ kcal} \cdot \text{mol}^{-1}$ (red) to $+25.7 \text{ kcal} \cdot \text{mol}^{-1}$ (blue).

Regarding the model of a stacked dimer, DA, Figure 6 middle, among the six intermolecular CH-Br interactions, one can identify two complementary favorable electrostatic interactions between CH groups of one molecule towards a bromine atom of the other molecule. Among these stabilizing interactions two of them, located para- to each other, appear to be strong with the shortest CH...Br distance of 2.98 \AA which is close to the sum of the van der Waals radii of H and Br (2.95 \AA). The four other interactions of this kind are weaker with CH...Br distances amounting to ca. 3.30 \AA . In the calculated model of dimer B (bottom of Figure 6) with two vicinal molecules, only one complementary lateral CH...Br interaction is found with a distance of 3.09 \AA . The interaction between the vicinal bromine atoms (3.95 \AA apart) should be destabilizing if the molecules were rigorously in the same plane. This may explain why the two molecules are slightly tilted and do not lie in the same plane.

Energy of formation of dimers or trimers of TXM calculated using atom-atom interactions

The initial model assumed that the molecules are rigid and that the effects of internal vibrations are neglected. This approximation is justified by the fact that we will take into account the structures found at temperatures below 15 K, so that even the lowest internal vibrational modes and lattice modes are sources of very small thermal amplitudes motions, except perhaps for the methyl hindered rotations. In fact, it is admitted that the Born-Oppenheimer approximation is valid for all the nuclei, *i.e.* that the localization of all the nuclei is well defined in agreement with neutron diffraction results. Then, it is assumed that the interactions between the molecules in the crystal can be represented as the sum of atom-atom terms, functions of the distance d_{ij} between atomic nuclei i and j and, for simplicity, it will be admitted that these radial interactions are isotropic. In the present work, it will be assumed that the main inter-atomic interaction potential is represented by the simple Buckingham or 'exp-6' potential of Equation 1 as in references [36-43] and in consequence the forces interacting between atoms i and j are given by Equation 2:

$$\text{Equation 1} \quad V_{ij} = K_{ij} \left\{ -A_{ij} / d_{ij}^6 + B_{ij} \exp(-C_{ij} d_{ij}) \right\}$$

$$\text{Equation 2} \quad F_{ij} = -\partial V_{ij} / \partial d_{ij} = K_{ij} \left\{ -6 A_{ij} / d_{ij}^7 + B_{ij} C_{ij} \exp(-C_{ij} d_{ij}) \right\}$$

In this approximation for non-polar molecules, there is no need to evaluate local atomic charges [36, 40] and so the convergence problems connected with the use of coulombic potential are avoided. The reasons to admit such simplification are: **1-** the parameters in Equation 1 which were deduced from the literature [43] have allowed to calculate accurately a lot of physical properties for several hundreds of molecular crystals, **2-** several sets of parameters may be used after small adjustments in order to better represent the cell parameters, **3-** the coefficient K_{ij} allows to adapt the value of the calculated energy to that of the sublimation energy if it has been measured **4-** the halogeno-mesitylenes are hexapolar molecules with local atomic net charges smaller than 0.3 electron from DFT computations, so that multipolar interactions are more or less included in parameters of Equation 1.

Table 4- Atom-atom 'exp-6' UNI van der Waals interaction coefficients^a used for the calculation of the energy of packing in the halogeno-methylbenzenes in the triclinic crystal phase.

| | TCM | | | | TBM | | | | TIM | | | |
|-------------|-------|-------|--------|------|-------|--------|---------|-------|-------|-------|---------|------|
| | At-at | Aij | Bij | Cij | At-at | Aij | Bij | Cij | At-at | Aij | Bij | Cij |
| UNI mean | Cl-Cl | -7939 | 950430 | 3.51 | Br-Br | -15180 | 1132190 | 3.28 | I-I | 35033 | 1560214 | 3.03 |
| | C-C | -2418 | 226145 | 3.47 | C-C | -2418 | 226145 | 3.47 | C-C | -2418 | 226145 | 3.47 |
| | H-H | -109 | 24158 | 4.01 | H-H | -109 | 24158 | 4.01 | H-H | -109 | 24158 | 4.01 |
| | Cl-C | -4382 | 463611 | 3.49 | Br-C | -6058 | 506003 | 3.375 | I-C | -9204 | 594000 | 3.25 |
| | Cl-H | -930 | 152845 | 3.76 | Br-H | -1287 | 165183 | 3.645 | I-H | -1954 | 194143 | 3.52 |
| | C-H | -513 | 73915 | 3.74 | C-H | -513 | 73915 | 3.74 | C-H | -513 | 73915 | 3.74 |

^aUnits: Aij (kJ/mol Å⁶), Bij (kJ/mol) and Cij (Å⁻¹)

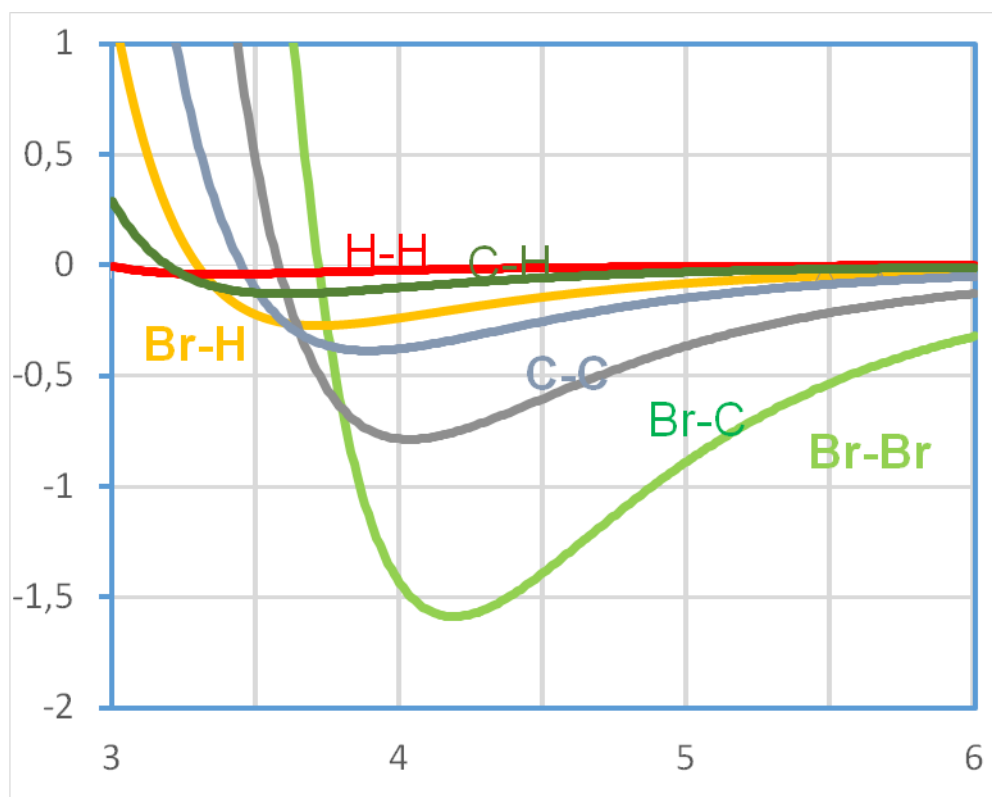


Figure 7- Variation of the atom-atom interaction forces as a function of the interatomic distance

Figure 7 illustrates for a pair of bromine atoms, the variation of the vdW interaction potential and of the corresponding force in function of the interaction distance d_{BrBr} ; they are calculated using Equations 1 and 2 respectively with $K_{ij} = 1$ and the “UNI” parameters given in Table 4 and the X-ray data.

Table 5- Bonding energy: UNI results for TBM^{a)}

| DA(M_p+M_+) | DA(M_p+M_-) | TA($M_- + M_p + M_+$) | DB(M_p+M_a) | DB(M_p+M_c) | TB ($M_a + M_p + M_c$) | HB ($M_p+ 6M$) ^{b)} |
|-----------------|-----------------|-------------------------|-----------------|-----------------|--------------------------|--------------------------------|
| -44.7 | -44.8 | -89.4 | -4.0 | -3.9 | -7.9 | -22.2 |

a) Energies in kJ/mol; b) HB: hexamer planar cluster, M_p has six neighbors in the **bc** plane.

As it can be seen in Table 5, the same conclusions as those obtained using DFT computations are reached using the empirical model, namely that the most stable stacking is obtained when the molecules are piled along axis **a**. An additivity rule applies for the bonding energies.

Finally, it can be seen that the order of magnitude of the computed stabilization energies is the same for the DFT and the empirical model approaches (Table 6) thus validating the theoretical approaches used here.

Table 6- Comparison between DFT and atom-atom energies (kJ/mol)

| | TBM (ω B97XD) | TBM (UNI) |
|------------------|-----------------------|-----------|
| $E_{DA} - 2.E_m$ | -55.1 | -44.8 |
| $E_{DB} - 2.E_m$ | -7.9 | -4.0 |
| E_{TA} | -115.5 | -89.4 |

Conclusions :

Below 300 K, trihalogeno mesitylene (TXM) molecules lead to needle shaped crystals in a triclinic arrangement. To shed light on the origin of such packing mode, we investigated different possible packings using two theoretical approaches, namely DFT computations and an empirical atom-atom interaction model. Thus, we considered aggregates of TXM molecules differently packed, namely dimers and trimers, and computed their packing energies. For the dimers and trimers of type A, the molecules are stacked one over the other along the **a** axis whereas dimer B and trimer B correspond to molecules lying in the **bc** plane.

From the DFT computations it appears that the stabilizing energy of formation of a dimer of two molecules stacked on top of each other along **a** is several times larger than the energy gain obtained for the formation of a dimer of two neighbors in the **bc** plane with edge-to-edge contacts. Moreover it has been found that the energy of formation of a trimer of type A is approximately twice the energy of formation of a dimer A so that an additive rule occurs. The main stabilizing effect which determines the crystal packing is the π - π stacking although consideration of the ESP maps in the case of TBM brings to light Br...H and Br...Br specific interactions.

The calculations using the empirical model leads to the same conclusions; these empirical calculations which may be extended to clusters of more numerous molecules along **a** or in the **bc** plane, demonstrate that the stabilizing energy of uni-dimensional stacking of TXM molecules like pancakes along the axis **a** is larger than that involved to form triangular interactions into a two-dimensional sheet. These conclusions are consistent with the experimental observations of the shape of the crystals obtained by crystallization from a super-saturated solution of TXM in an organic solvent: long crystalline needles aligned along the axis **a** are always obtained and never thin dimensional sheets.

Acknowledgements:

We acknowledge the HPC resources of CINES and of IDRIS under the allocations 2017 and 2018 [x2016080649] made by GENCI (Grand Equipement National de Calcul Intensif).

Experimental part:

Differential scanning calorimetry (DSC) was carried out by using NETZSCH DSC 200 F3 instrument equipped with an intracooler. Temperature dependent XRD analysis were performed on a D8 VENTURE Bruker AXS diffractometer operating with graphite-monochromated Mo-K α radiation ($\lambda =$

0.71073 Å). Optical microscopy investigations were performed on a Nikon H600L polarizing microscope equipped with a Linkam "liquid crystal pro system" hotstage LTS420.

References:

- [1] A. H. White, B. S. Biggs and S. O. Morgan, *J. Am. Chem. Soc.* **1940**, 62, 16
- [2] A. Tulinsky and J. G. White, *Acta Cryst.* **1958**, 11, 7
- [3] G. Charbonneau and J. Meinel, *J. Chimie Phys. & Radium*, **1968**, 65, 1590
- [4] G. Charbonneau and Trotter, *J. Chem. Soc. A*, **1967**, 2032; *ibid.* **1968**, 1267
- [5] J. C. Messenger, H. Cailleau and W. Yellon, *Acta Cryst.* **1978**, A34, 384
- [6] D. André, R. Fourme and M. Renaud, *Acta Cryst. B*, **1971**, 27, 2371
- [7] Y. Balcou and J. Meinel. *J. Chimie Phys.* **1966**, 62, 114
- [8] M. Eveno and J. Meinel, *J. Chimie Phys.* **1966**, 62, 108
- [9] C. Brot and I. Darmon, *J. Chimie Phys.* **1966**, 63, 100; C. Brot and I. Darmon. *J. Chem. Phys.* **1970**, 53, 2271
- [10] R. Fourme, M. Renaud and D. André, *Molecular and Liquid Crystals* **1972**, 17, 209
- [11] A. Kitaigorodski, *Molecular Crystals and Molecules*, *Academic Press* **1973**
- [12] M. Tazi, J. Meinel, M. Sanquer, M. Nusimovici, F. Tonnard and R. Carrié, *Acta Cryst B*, **1995**, 37, 838
- [13] F. Boudjada, J. Meinel, A. Cousson, W. Paulus, M. Mani and M. Sanquer, *AIP CP479-N2M*, **1999**, 217
- [14] J. Meinel, M. Mani, A. Cousson, F. Boudjada, W. Paulus and M. Johnson, *Chem. Phys.* **2000**, 261, 165
- [15] A. Boudjada, O. Hernandez, J. Meinel, M. Mani and W. Paulus, *Acta Cryst. C*, **2001**, 57, 1106
- [16] A. Boudjada, J. Meinel, A. Boucekkine, O. Hernandez and M-T. Fernandez-Diaz, *J. Chem. Phys.*, **2002**, 117, 10173
- [17] E. Bosch and C. L. Barnes, *Crystal Growth & Design*, **2002**, 2, 299
- [18] O. Hernandez, K. S. Knight, W. Van Beck, A. Boucekkine, A. Boudjada, W. Paulus and J. Meinel, *J. Mol. Structure*, **2006**, 791, 41
- [19] S. Takeda, T. Fujiwara, H. Chihara, *J. Phys. Soc. Jpn*, **1989**, 58, 1793
- [20] T. Fujiwara, T. Atake, H. Chihara, *Bull. Chem. Soc. Jpn*, **1990**, 63, 657

- [21] G. R. Desiraju, Crystal Engineering. *The design of organic solids*. Science Monographs, 54. Elsevier **1989**.
- [22] C. M. Reddy, M.T. Kirchner, R. C. Gundakaram, K. A. Padmanabham and G. R. Desiraju, *Chem. Eur. J.* **2006**, *12*, 2222
- [23] S. L. Price, A. J. Stone, J. Lucas, R. J. Rowland and A. E. Thornley, *J. Am. Chem. Soc.* **1994**, *116*, 4910
- [24] B. S. Green and G. M. Schmidt, *Israel Chem. Soc. Annual meetings abstracts*, **1971**, 190
- [25] G. R. R. J. Desiraju and Parthasarathy, *J. Am. Chem. Soc.* **1989**, *111*, 8725
- [26] S. C. Nyburg and C. H. Faerman, *Acta Cryst. B*, **1985**, *41*, 274
- [27] F. F. Awwadi, R. D. Willet, K. A. Peterson and B. Twamley, *Chem. Eur. J.* **2006**, *12*, 8952
- [28] P. Politzer, P. Lane, M. C. Concha, Y. Ma and J. S. Murray, *J. Mol. Model*, **2007**, *13*, 305
- [29] P. Auffinger, F. Hays, E. Westhof and P. S. Ho, *Proc. Natl Acad. Sci. USA* **2004**, *101*, 16789
- [30] (a) M. Fourmigué and P. Batail, *Chem. Rev.* **2004**, *104*, 5379; (b) *Halogen Bonding. Fundamentals and Applications*. P. Metrangolo and G. Resnati editors. Springer 2008; (c) M. Fourmigué, *Current Opinion in Solid State and Materials Science*, **2009**, *13*, 36
- [31] R. Peverati and D.G. Truhlar, *Phil. Trans. R. Soc.* **2014**, *A 372*, 20120476.
- [32] A.D. Becke, *J. Chem. Phys.* **2014**, *140*, 18A301.
- [33] J.-D. Chai and M. Head-Gordon, *Phys. Chem. Chem. Phys.* **2008**, *10*, 6615.
- [34] P. J. Hay and W. R. Wadt, *J. Chem. Phys.* **1985**, *82*, 299
- [35] M. J. Frisch, G. W. Trucks, H. B. Schlegel, G. E. Scuseria, M. A. Robb, J. R. Cheeseman, G. Scalmani, V. Barone, B. Mennucci and G. A. Petersson, Gaussian09, 2015.
- [36] A.I. Kitaigorodsky and K.V. Mirskaya, *Soviet Phys. (Crystallogr.)* **1964**, *9*, 137.
- [37] D.E. Williams, *J. Chem. Phys.* **1967**, *47*, 4680.
- [38] J A. Warshel and S. Lifson, *J. Chem. Phys.* **1970**, *53*, 582.
- [39] A.I. Kitaigorodsky, *Molecular Crystals and Molecules*. Academic Press, 1973. p. 21, 22
- [40] D.E. Williams, *Acta Crystallogr. A* **1974**, *30*, 71.
- [41] A. I. Pertsin and A.I. Kitaigorodsky, *The Atom-Atom Potential Method*. Springer 1986

[42] A. Gavezzotti, *Molecular Aggregation* IUCr 2007

[43] G. Filippini and A. Gavezzotti, *Acta Cryst. B* **1993**, 49, 868.

ACCEPTED MANUSCRIPT

Highlights :

- . Trihalogeno mesitylene (TXM) molecules lead to needle shaped crystals in a triclinic arrangement.
- . Computed packings using DFT and an empirical atom-atom interaction model.
- . The stabilization energy for TXM piled up molecules is the highest one.
- . Electrostatic potential maps bring light on X...X and X...H specific interactions.